

LETTER • OPEN ACCESS

## Machine learning inference of molecular dipole moment in liquid water

To cite this article: Lisanne Knijff and Chao Zhang 2021 *Mach. Learn.: Sci. Technol.* **2** 03LT03

View the [article online](#) for updates and enhancements.

You may also like

- [Do molecular dipole interactions influence solid state organization?](#)  
J K Whitesell, R E Davis, L L Saunders et al.
- [Challenging chemical concepts through charge density of molecules and crystals](#)  
Carlo Gatti
- [Strong superchiral field in hot spots and its interaction with chiral molecules](#)  
Y. Liu, W. Zhao, Y. Ji et al.



## LETTER

## OPEN ACCESS

## RECEIVED

28 March 2021

## ACCEPTED FOR PUBLICATION

13 May 2021

## PUBLISHED

13 July 2021

Original Content from this work may be used under the terms of the [Creative Commons Attribution 4.0 licence](#).

Any further distribution of this work must maintain attribution to the author(s) and the title of the work, journal citation and DOI.



# Machine learning inference of molecular dipole moment in liquid water

Lisanne Knijff and Chao Zhang\*

Department of Chemistry-Ångström Laboratory, Uppsala University, Lägerhyddsvägen 1, BOX 538, 75121 Uppsala, Sweden

\* Author to whom any correspondence should be addressed.

E-mail: [chao.zhang@kemi.uu.se](mailto:chao.zhang@kemi.uu.se)**Keywords:** polarization surface, molecular dipole moment, graph convolution, charge model, molecular liquidsSupplementary material for this article is available [online](#)

## Abstract

Molecular dipole moment in liquid water is an intriguing property, partly due to the fact that there is no unique way to partition the total electron density into individual molecular contributions.

The prevailing method to circumvent this problem is to use maximally localized Wannier functions, which perform a unitary transformation of the occupied molecular orbitals by minimizing the spread function of Boys. Here we revisit this problem using a data-driven approach satisfying two physical constraints, namely: (a) The displacement of the atomic charges is proportional to the Berry phase polarization; (b) Each water molecule has a formal charge of zero. It turns out that the distribution of molecular dipole moments in liquid water inferred from latent variables is surprisingly similar to that obtained from maximally localized Wannier functions. Apart from putting a maximum-likelihood footnote to the established method, this work highlights the capability of graph convolution based charge models and the importance of physical constraints on improving the model interpretability.

Molecular dipole moment in polar liquids, such as liquid water, is an intriguing property [1]. On one hand, its magnitude and variation are directly linked to the dielectric properties of polar liquids and the intensities in infrared and sum-frequency generation spectra; On the other hand, molecular dipole moment in polar liquids is not accessible to direct measurement.

One prominent example of using molecular dipole moment is the Kirkwood theory of the static dielectric constant  $\epsilon$  in polar liquids [2], which directly involves the mean value of the molecular dipole in the liquid, i.e.  $\langle\mu\rangle$ , and the orientational correlation factor, i.e. the Kirkwood g-factor  $g_K$  [3].

$$\frac{(\epsilon - 1)(2\epsilon + 1)}{\epsilon} = 4\pi\beta\rho\langle\mu\rangle^2 g_K \quad (1)$$

where  $\rho$  and  $\beta$  are the number density and the inverse temperature respectively. In his 1939 paper, [2] Kirkwood noticed that scaling the gas phase dipole of a water molecule by a factor of 1.26 may lead to an exact agreement on  $\epsilon$  with the experiments and attributed this to a strong polarization effect by neighboring molecules in the liquid phase.

The most notable estimation of the molecular dipole of water was given by Coulson and Eisenberg with an induction model in 1966 [4]. They found that the reaction field from neighboring molecules in ice  $I_h$  increases the molecular dipole to about 2.6 D, compared to 1.84 D of an isolated  $H_2O$  molecule. This issue was revisited in 1999 [5]. Instead of partitioning the total electron density of liquid water to individual water molecules [6], Silvestrelli and Parrinello found that  $\langle\mu\rangle$  is about 3.0 D by using density functional theory based molecular dynamics (DFTMD) [7] and maximally localized Wannier functions (MLWFs) [8]. Their result agrees with the reanalysis of the Coulson-Eisenberg model [9] and implies a charge transfer of about 0.5e along each O–H bond [10, 11].

In MLWFs, [8] the Boys localization [12] was employed to maximize the distance between centroids of orbitals (Wannier centers). However, alternative localization schemes are possible [13]. In a recent work, [14] Edmiston-Ruedenberg localization [15], which maximizes the self-repulsion energy of orbitals, has been explored to investigate the molecular dipole moment in liquid water. Depending on the regularization parameter, the resulting  $\langle \mu \rangle$  varies between 2.35 D and 2.63 D [14].

In this work, we tackle this issue with a physically constrained data-driven approach. Similar to the dipole moment of an isolated molecule, the change in polarization  $\Delta \mathbf{P}$  in condensed phase systems is well defined and experimentally measurable [16]. For liquid water, with the choice of the molecular gauge,  $\mathbf{P}$  is the so-called itinerant polarization [17]. This is the target quantity that we used in the regression task for liquid water. In contrast, molecular dipole moments here are inferred from latent variables and not involved in the training of the model. Another physical constraint built into our regression model is the charge neutrality of each water molecule, which is formally required by the integer change of the polarization quantum in the modern theory of polarization [18, 19]. Taking these ingredients into account, we show that the distribution of molecular dipole moments inferred from our regression model using the graph convolutional neural network architecture PiNet is surprisingly similar to that obtained from MLWFs. Moreover, the trained model, with PiNet using only data at ambient conditions, is transferable to liquid water in a range of different densities.

The loss function  $\mathcal{L}$  that we used for predicting the itinerant polarization  $\mathbf{P}$  is the squared error in terms of the  $l^2$  norm:

$$\mathcal{L} = \sum_i^n \|\mathbf{R}_i \mathbf{Q}_i - \mathbf{P}_i \Omega\|_2^2 \quad (2)$$

where  $\mathbf{R}_i$  is a  $3 \times N$  matrix of the atomic coordinates of the configuration  $i$  for a system containing  $N$  atoms.  $\mathbf{Q}_i$  represents a column vector of the atomic charge in the configuration  $i$ .  $\Omega$  is the volume of the simulation box.

In our ML model, neutrality is enforced for each water molecule. This is done by subtracting the net charge using the following expression:

$$\mathbf{Q}_i = \bigoplus_{j=1}^{N_w} \left( \mathbf{Q}_{ij} - \frac{\mathbf{J}^T \mathbf{Q}_{ij} \mathbf{J}}{3} \right) \quad (3)$$

where  $N_w$  is the number of water molecules in the system,  $\mathbf{J}$  is a column vector with each entry equal to one, and  $\bigoplus$  is used as the symbol for the concatenation of vectors.

The loss function in equation (2) was trained with PiNet, a high-performing graph convolutional neural network architecture which works for both isolated molecules and condensed phase systems [20]. Despite the simplicity of our scalar dipole model, PiNet leads to an outstanding learning curve with the QM9 dataset [21], compared to even more sophisticated models [22] (see figure 1(a)). For liquid water, the itinerant polarization  $\mathbf{P}$  was computed with the CP2K package [23] and the BLYP functional [24, 25] using the Berry phase formula [26] (see equation (S1)). In this case, the PiNet-dipole model gives an excellent prediction of  $\|\mathbf{P}\Omega\|$  with a mean absolute error (MAE) of 0.037 D for the test set (see figure 1(b)). Here we followed the conventional 80:20 splitting of the dataset (see electronic supplementary information (available online at [stacks.iop.org/MLST/2/03LT03/mmedia](https://stacks.iop.org/MLST/2/03LT03/mmedia)) for further descriptions of the computational methods and the dataset).

Before looking into the inferred molecular dipole moment in liquid water from the PiNet-dipole model, it is necessary to set up a baseline for the sake of comparison. The baseline model used here is the linear regression (LR)-dipole model.

Equation (2) resembles a LR problem where  $\mathbf{Q}$  may be considered as the weight vector. However, this requires the configuration-dependent  $\mathbf{Q}_i$  to be substituted by the configuration-independent  $\bar{\mathbf{Q}}$ . This leads to the loss function used in the LR-dipole model as

$$\mathcal{L} = \sum_i^n \|\mathbf{R}_i \bar{\mathbf{Q}} - \mathbf{P}_i \Omega\|_2^2 + \lambda \sum_j^{N_w} \|\mathbf{\Gamma}_j \bar{\mathbf{Q}}\|_2^2 \quad (4)$$

where Tikhonov matrices  $\mathbf{\Gamma}$  are introduced to ensure the charge neutrality of each water molecule and  $\lambda$  is the ridge parameter. For example, if the first three entries in  $\bar{\mathbf{Q}}$  are  $\{q_O, q_H, q_H\}$  for one water molecule, then  $\mathbf{\Gamma}_j$  can be written as:

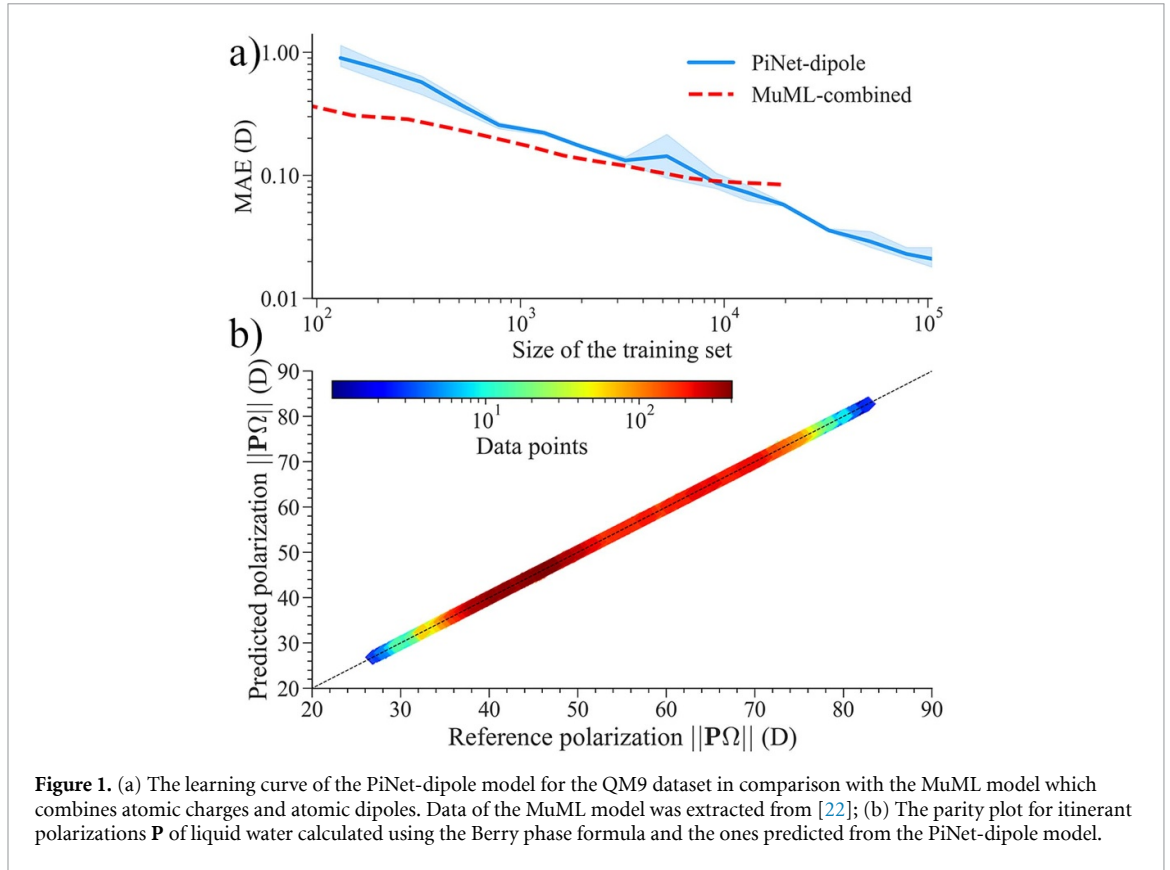


**Figure 1.** (a) The learning curve of the PiNet-dipole model for the QM9 dataset in comparison with the MuML model which combines atomic charges and atomic dipoles. Data of the MuML model was extracted from [22]; (b) The parity plot for itinerant polarizations  $\mathbf{P}$  of liquid water calculated using the Berry phase formula and the ones predicted from the PiNet-dipole model.

**Table 1.** The comparison between the linear regression (LR)-dipole model and the PiNet-dipole model for predicting the itinerant polarization  $\mathbf{P}$  of liquid water in terms of the root mean square error (RMSE) and the mean absolute error (MAE). Entries are  $\|\mathbf{P}\Omega\|$  in Debye (D). CN means applying the charge neutrality constraint for each water molecule.

Method	RMSE	MAE
LR-dipole (without CN)	1.996	1.609
LR-dipole	2.033	1.632
PiNet-dipole (without CN)	0.212	0.164
PiNet-dipole	0.054	0.037

$$\mathbf{\Gamma}_j = \begin{bmatrix} 1 & 1 & 1 & 0 & \cdots \\ 0 & 0 & 0 & 0 & \cdots \\ \vdots & \vdots & \vdots & \vdots & \vdots \end{bmatrix}. \quad (5)$$

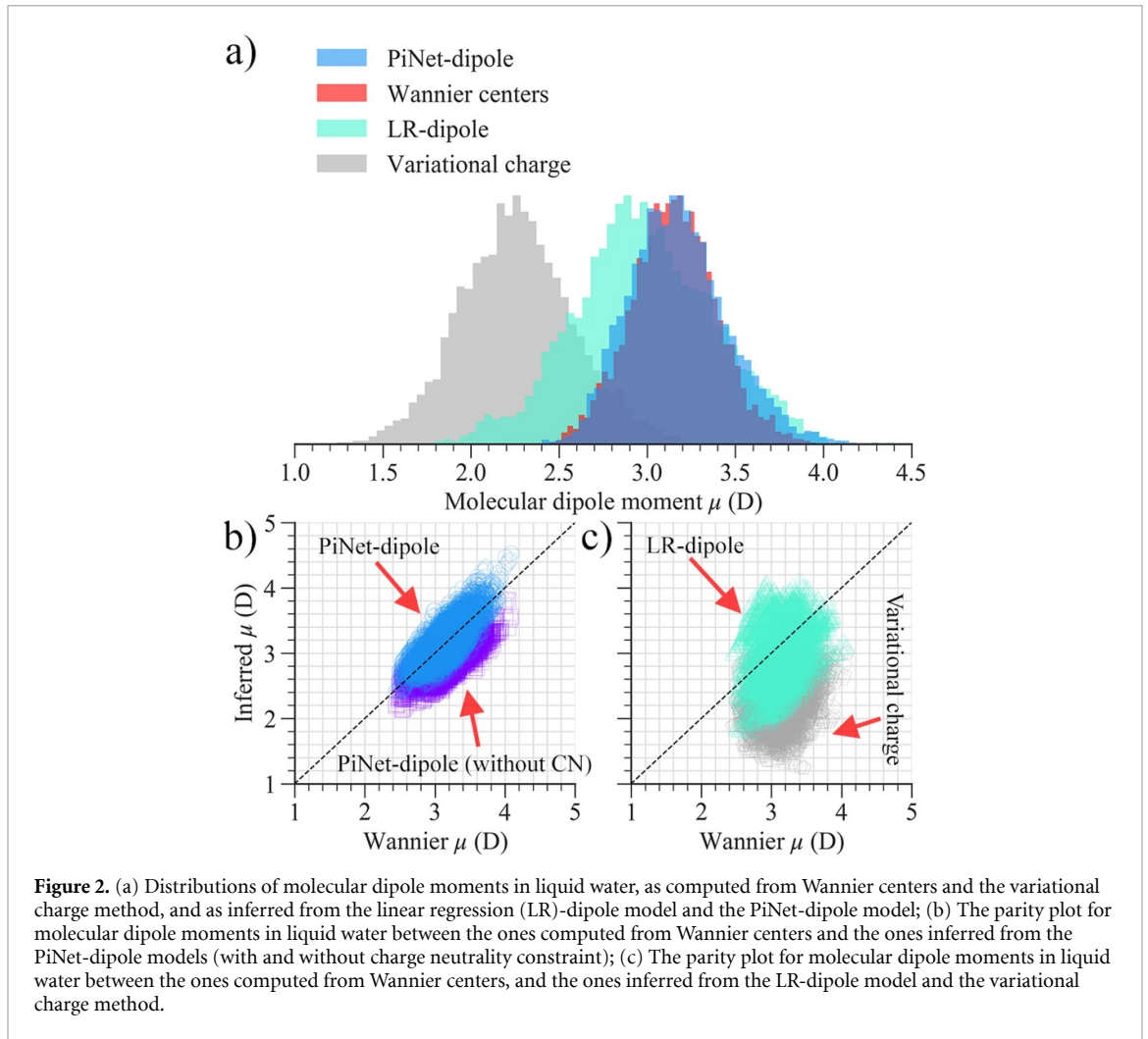
Therefore, the corresponding optimal solution for  $\bar{\mathbf{Q}}^*$  is:

$$\bar{\mathbf{Q}}^* = \left( \mathbf{R}^T \mathbf{R} + \lambda \sum_j^{N_w} \mathbf{\Gamma}_j^T \mathbf{\Gamma}_j \right)^{-1} \mathbf{R}^T \mathbf{P}\Omega. \quad (6)$$

Note that here the subscript  $i$  is dropped and that  $\mathbf{R}$  includes all the input data over three Cartesian coordinates, which make it a  $3n \times N$  matrix instead.

As seen in table 1, the itinerant polarization of liquid water predicted from the PiNet-dipole model is orders of magnitude more accurate than that predicted using the LR-dipole model. Moreover, the PiNet-dipole model with charge neutrality constraint performs significantly better than the one without charge neutrality constraint. These highlight the necessity of having environmental-dependent atomic charges built into the PiNet-dipole model and to impose physical constraints which are compatible with the modern theory of polarization.

Now we are ready to compare the molecular dipole moments in liquid water as inferred from the PiNet-dipole model with those inferred from the linear regression dipole model. To put this comparison into perspective, we included the ones computed with Wannier centers from MLWFs (see equation (S2)). The reference calculations of the Wannier dipole moments were done with the same computational setup as the



one used in computing the itinerant polarization  $\mathbf{P}$  (see electronic supplementary information for details). Results of this comparison are given in figure 2.

The most interesting finding in figure 2(a) is that the distribution of molecular dipole moments in liquid water inferred from the PiNet-dipole model is very close to that computed with Wannier centers. Since there is no regularization term in equation (2), this result may be seen as a maximum-likelihood footnote to MLWFs. In this regard, the LR-dipole model is quite off. In addition, as shown in figure 2(b), the charge neutrality constraint is an important factor to achieve a good correlation. Because reproducing the itinerant polarization of liquid water and retaining the charge neutrality for each water molecule are two main ingredients in the PiNet-dipole model, the question that naturally arises is whether methods which satisfy these two conditions will necessarily lead to molecular dipole moments which are close to the ones obtained with Wannier centers in MLWFs.

Instead of viewing equation (2) as a regression problem, one may use reference charges  $\mathbf{Q}^\circ$  to supplement the equation and transform it to a set of linear equations [27, 28]. This approach is what we call the variational charge method here, as the loss function shown below may be viewed as an energy functional with respect to the atomic charge  $\mathbf{Q}_i$ .

$$\mathcal{L} = \epsilon^\top (\mathbf{R}_i \mathbf{Q}_i - \mathbf{P}_i \Omega) + \frac{\kappa}{2} \|\mathbf{Q}_i - \mathbf{Q}_i^\circ\|_2^2 + \boldsymbol{\eta}^\top \left( \sum_j^{N_w} \boldsymbol{\Gamma}_j \mathbf{Q}_i \right) \quad (7)$$

where  $\epsilon$  is a column vector which plays the role of a Lagrange multiplier and  $\kappa$  is a weight parameter. To introduce charge neutrality for each water molecule, we added a third term in equation (7) where  $\boldsymbol{\eta}$  is a Lagrange multiplier and  $\boldsymbol{\Gamma}_j$  is the same Tikhonov matrix as given in equation (5).

Taking the derivative of equation (7) with respect to  $\mathbf{Q}_i$ ,  $\epsilon$  and  $\boldsymbol{\eta}$  leads to a set of  $N + 3 + N/3$  linear equations:

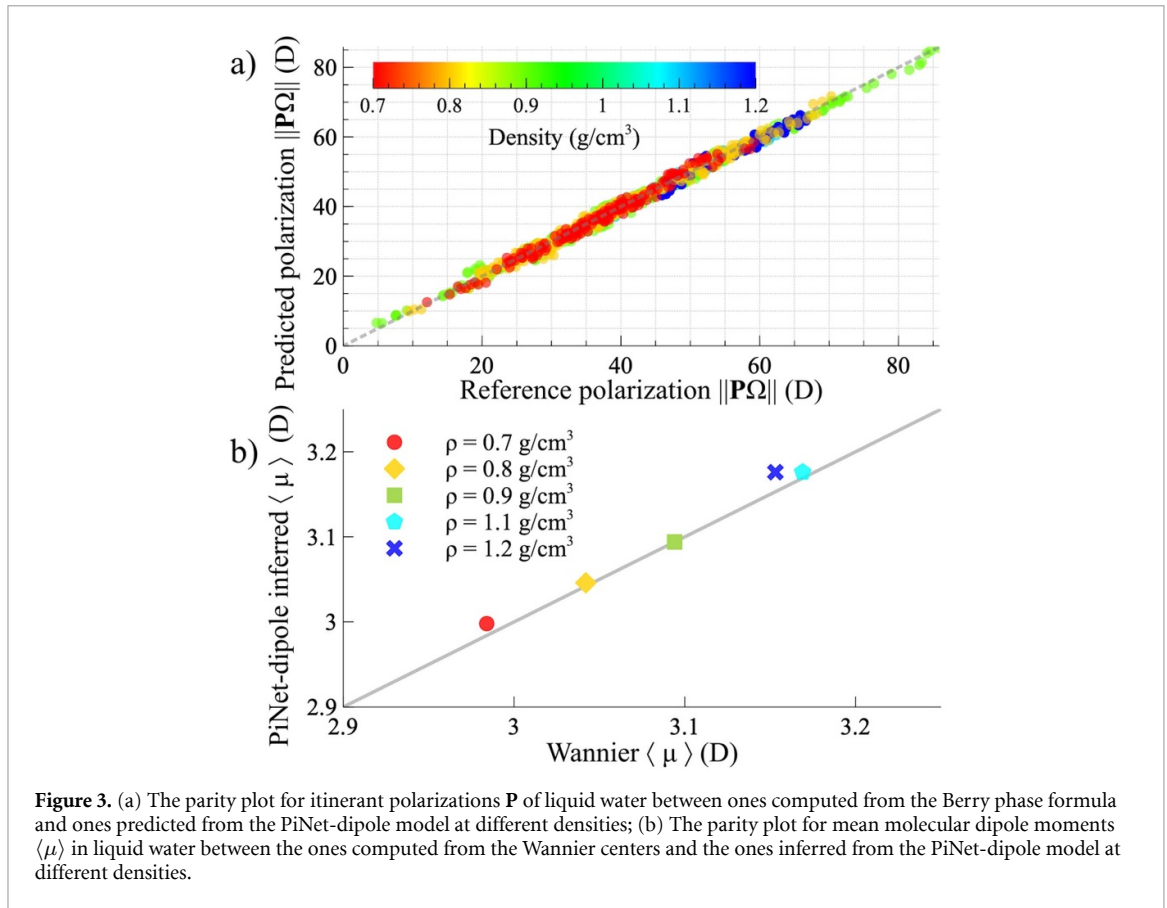


**Figure 3.** (a) The parity plot for itinerant polarizations  $\mathbf{P}$  of liquid water between ones computed from the Berry phase formula and ones predicted from the PiNet-dipole model at different densities; (b) The parity plot for mean molecular dipole moments  $\langle \mu \rangle$  in liquid water between the ones computed from the Wannier centers and the ones inferred from the PiNet-dipole model at different densities.

$$\begin{bmatrix} \kappa \mathbf{I} & \mathbf{R}_i^\top & \sum_j^{N_w} \mathbf{\Gamma}_j^\top \\ \mathbf{R}_i & 0 & 0 \\ \sum_j^{N_w} \mathbf{\Gamma}_j & 0 & 0 \end{bmatrix} \begin{bmatrix} \mathbf{Q}_i \\ \epsilon \\ \eta \end{bmatrix} = \begin{bmatrix} \kappa \mathbf{Q}_i^\circ \\ \mathbf{P}_i \Omega \\ 0 \end{bmatrix} \quad (8)$$

where  $\mathbf{I}$  is a  $N \times N$  identity matrix. Note that equation (8) is solved independently for each configuration  $i$ .

The reference charges  $\mathbf{Q}^\circ$  for liquid water were obtained with the REPEAT method [29, 30], which provides electrostatic potential derived charges in periodic systems (see electronic supplementary information for details). Since both  $\epsilon$  and  $\eta$  in equation (7) are Lagrange multipliers, the two physical constraints mentioned before (reproducing the itinerant polarization and retaining the charge neutrality) are exactly satisfied in the variational charge method. However, as shown in figures 2(a) and (c), the resulting molecular dipole moments are very different from the ones obtained with Wannier centers. This suggests that one should not take the striking agreement between the molecular dipole moments in liquid water inferred from the PiNet-dipole model and those computed with Wannier centers for granted. The effective inclusion of long-range charge transfer in graph convolution [31] is likely to be the reason behind this, because the delocalization tail along the hydrogen bonds contributes significantly to the molecular dipole moment in water clusters [32].

Finally, how good is the transferability of the PiNet-dipole model for liquid water? To answer that, we used a publicly accessible dataset for BLYP liquid water at different densities [33, 34]. Results of the predicted itinerant polarizations  $\mathbf{P}$  and the corresponding mean molecular dipole moments  $\langle \mu \rangle$  are shown in figure 3. Despite the fact that the PiNet-dipole model was trained using data only at ambient conditions (i.e.  $\rho = 1.0 \text{ g cm}^{-3}$ ), this model is rather transferable for liquid water in a range of different densities (figure 3(a)). Moreover, the mean water dipole moments  $\langle \mu \rangle$  at different densities as inferred from the PiNet-dipole model correlate quite well with those calculated from the Wannier centers (figure 3(b)). These excellent agreements may be due to the high expressiveness of the underlying graph convolutional neural network architecture PiNet [20], which is also seen in the learning curve shown in figure 1(a) for isolated molecules.

Presumably, the paradigm in atomistic machine learning at present focuses on predicting physical quantities which enter into the loss function and the model training, e.g. energy, force and charge [35–37]. Instead, we looked into the latent variables of a trained network in this work and showed that the molecular dipole moments in liquid water inferred from the PiNet-dipole model are surprisingly in accord with those

obtained from Wannier centers. Apart from the importance of physical constraints as shown in this work, future studies should investigate other factors which could contribute to this agreement, e.g. an effective inclusion of long-range charge transfer. With these efforts, graph convolution based charge models could provide an alternative for describing the itinerant polarization in condensed phase systems [38]. Thus, their applications to charged systems, such as electrolyte materials and electrified solid-liquid interfaces [39, 40], shall be anticipated.

### Data availability statement

The polarization dataset for liquid water can be accessed using the following link <https://doi.org/10.5281/zenodo.4752246>. Other data that support the findings of this study are included within the article (and any supplementary files).

### Acknowledgments

This project has received funding from the European Research Council (ERC) under the European Union's Horizon 2020 research and innovation programme (Grant No. 949012). L K is partly supported by a PhD studentship from the Centre for Interdisciplinary Mathematics (CIM) at Uppsala University. The calculations were performed on the resources provided by the Swedish National Infrastructure for Computing (SNIC) at UPPMAX and PDC.

### ORCID iD

Chao Zhang  <https://orcid.org/0000-0002-7167-0840>

### References

- [1] Debye P J W 1929 *Polar Molecules* (New York: Dover Publications)
- [2] Kirkwood J G 1939 *J. Chem. Phys.* **7** 911
- [3] Zhang C, Hutter J and Sprik M 2016 *J. Phys. Chem. Lett.* **7** 2696–701
- [4] Coulson C A and Eisenberg D 1966 *Proc. R. Soc. A* **291** 445–53
- [5] Silvestrelli P and Parrinello M 1999 *Phys. Rev. Lett.* **82** 3308–11
- [6] Site L D, Alavi A and Lynden-Bell R M 1999 *Mol. Phys.* **96** 1683–93
- [7] Car R and Parrinello M 1985 *Phys. Rev. Lett.* **55** 2471–4
- [8] Marzari N and Vanderbilt D 1997 *Phys. Rev. B* **56** 12847–65
- [9] Batista E R, Xantheas S S and Jónsson H 1998 *J. Chem. Phys.* **109** 4546–51
- [10] Badyal Y S, Saboungi M L, Price D L, Shastri S D, Haeffner D R and Soper A K 2000 *J. Chem. Phys.* **112** 9206–8
- [11] Liu H, Wang Y and Bowman J M 2016 *J. Phys. Chem. B* **120** 1735–42
- [12] Foster J M and Boys S F 1960 *Rev. Mod. Phys.* **32** 300–2
- [13] Löwdin P O 1966 *Quantum Theory of Atoms, Molecules and the Solid State: A Tribute to J.C. Slater* (New York: Academic Inc)
- [14] Zhu T and Van Voorhis T 2020 *J. Phys. Chem. Lett.* **6**–12
- [15] Edmiston C and Ruedenberg K 1963 *Rev. Mod. Phys.* **35** 457–64
- [16] Resta R and Vanderbilt D 2007 *Theory of Polarization: A Modern Approach Physics of Ferroelectrics* (Berlin: Springer) pp 31–68
- [17] Caillol J M 1994 *J. Chem. Phys.* **101** 6080–12
- [18] King-Smith R and Vanderbilt D 1993 *Phys. Rev. B* **47** 1651–4
- [19] Resta R 1994 *Rev. Mod. Phys.* **66** 899–915
- [20] Shao Y, Hellström M, Mitev P D, Knijff L and Zhang C 2020 *J. Chem. Inf. Model.* **60** 1184–93
- [21] Ramakrishnan R, Dral P O, Rupp M and von Lilienfeld O A 2014 *Sci. Data* **1** 140022
- [22] Veit M, Wilkins D M, Yang Y, DiStasio R A and Ceriotti M 2020 *J. Chem. Phys.* **153** 1–15
- [23] Hutter J, Iannuzzi M, Schiffmann F and VandeVondele J 2013 *WIREs Comput. Mol. Sci.* **4** 15–25
- [24] Becke A D 1988 *Phys. Rev. A* **38** 3098–100
- [25] Lee C, Yang W and Parr R G 1988 *Phys. Rev. B* **37** 785–9
- [26] Resta R 1998 *Phys. Rev. Lett.* **80** 1800–3
- [27] Laio A, Gervasio F L, VandeVondele J, Sulpizi M and Rothlisberger U 2004 *J. Phys. Chem. B* **108** 7963–8
- [28] Kirchner B and Hutter J 2004 *J. Chem. Phys.* **121** 5133–11
- [29] Campaná C, Mussard B and Woo T K 2009 *J. Chem. Theory Comput.* **5** 2866–78
- [30] Golze D, Hutter J and Iannuzzi M 2015 *Phys. Chem. Chem. Phys.* **17** 14307–16
- [31] Zubatyuk R, Smith J S, Leszczynski J and Isayev O 2019 *Sci. Adv.* **5** eaav6490
- [32] Bakó I and Mayer I 2016 *J. Phys. Chem. A* **120** 4408–17
- [33] Morawietz T and Behler J 2019 HDNNP training data set for H<sub>2</sub>O (<https://zenodo.org/record/2634098>)
- [34] Morawietz T, Singraber A, Dellago C and Behler J 2016 *Proc. Natl. Acad. Sci. USA* **113** 8368–73
- [35] Bartók A P, De S, Poelking C, Bernstein N, Kermode J R, Csányi G and Ceriotti M 2017 *Sci. Adv.* **3** e1701816
- [36] Aspuru-Guzik A, Lindh R and Reiher M 2018 *ACS Cent. Sci.* **4** 144–52
- [37] Lilienfeld O A, Müller K R and Tkatchenko A 2020 *Nat. Rev. Chem.* **4** 347–58
- [38] Zhang L, Chen M, Wu X, Wang H, E W and Car R 2020 *Phys. Rev. B* **102** 041121
- [39] Zhang C, Sayer T, Hutter J and Sprik M 2020 *J. Phys. Energy* **2** 032005
- [40] Shao Y, Knijff L, Dietrich F M, Hermansson K and Zhang C 2021 *Batteries Supercaps* **4** 585–95